17. P. Vainikainen, J. Ollikainen, O. Kivekäs, and I. Kelander, Resonator-based analysis of the combination of mobile handset antenna and chassis, IEEE Trans Antennas Propag 50 (2002), 1433–1444.
18. R. Hossa, A. Byndas, and M.E. Bialkowski, Improvement of compact terminal antenna performance by incorporating open-end slots in ground plane, IEEE Microwave Wireless Component Lett 14 (2004), 283–285.
19. M.F. Abedin and M. Ali, Modifying the ground plane and its effect on planar inverted-F antennas (PIFAs) for mobile phone handsets, IEEE Antennas Wireless Propag Lett 2 (2003), 226–229.
20. M. Cabedo-Fabrés, E. Antonino-Daviu, A. Valero-Nogueira, and M. Ferrando Bataller, The theory of characteristic modes revisited: A contribution to the design of antennas for modern applications, IEEE Antennas Propag Mag 49 (2007), 52–68.
21. W.L. Schroeder, C.T. Famdie, and K. Solbach, Utilization and tuning of the chassis modes of a handheld terminal for the design of multiband radiation characteristics, In: IEEE Wideband and Multiband Antennas and Arrays, September 2005, pp. 117–121.
22. J. Anguera, I. Sanz, A. Sanz, A. Condes, D. Gala, C. Puente, and J. Soler, Enhancing the performance of handset antennas by means of groundplane design, In: IEEE International Workshop on Antenna Technology: Small Antennas and Novel Metamaterials (iWAT 2006), New York, March 2006.
23. J. Anguera, A. Cabedo, C. Picher, I. Sanz, M. Ribó, and C. Puente, Multiband handset antennas by means of groundplane modification, In: IEEE Antennas and Propagation Society International Symposium, Honolulu, Hawaii, June 2007.
24. C. Picher, J. Anguera, A. Cabedo, C. Puente, and S. Kahng, Multiband handset antenna using slots on the ground plane: Considerations to facilitate the integration of the feeding transmission line, Prog Electromagn Res C 7 (2009), 95–109.
25. R. Quintero and C. Puente, Multilevel and space-filling ground planes for miniature and multiband antennas, Pat. Appl. WO2003/023900, September 13, 2001.
26. J. Anguera and C. Puente, Shaped ground plane for radio apparatus, Pat. Appl. WO2006/070017, December 29, 2005.
27. C. Puente and J. Anguera, Handset with electromagnetic bra, Pat. Appl. WO2005/083833, February 28, 2005.
28. J. Rahola and J. Ollikainen, Optimal antenna placement for mobile terminals using characteristic mode analysis, In: First European Conference on Antennas and Propagation, 2006, EuCAP 2006.
29. J. Villanen, J. Ollikainen, O. Kivekäs, and P. Vainikainen, Coupling element based mobile terminal antenna structures, IEEE Trans Antennas Propag 54 (2006), 2142–2153.
30. S. Ozden, B.K. Nielsen, C.H. Jorgensen, J. Villanen, C. Icheln, and P. Vainikainen, Quad-band coupling element antenna structure, U.S. Pat. 7,274,340, September 25, 2007.
31. J. Anguera, A. Andújar, C. Puente, and J. Mumbru, Antennaless wireless device, Pat. Appl. WO2010/015365, July 31, 2009.
32. J. Anguera, A. Andújar, C. Puente, and J. Mumbru, Antennaless wireless device capable of operation in multiple frequency regions, Pat. Appl. WO2010/015364, July 31, 2009.
33. A. Andújar, J. Anguera, and C. Puente, Ground plane boosters as a compact antenna technology for wireless handheld devices, IEEE Trans Antennas Propag 59 (2011), 1668–1677.
34. E.H. Newman, Small antenna location synthesis using characteristic modes, IEEE Trans Antennas Propag AP-27 (1979), 530–531.
35. R.J. Garbacz and R.H. Turpin, A generalized expansion for radiated and scattered fields, IEEE Trans Antennas Propag AP-19 (1971), 348–358.
36. R.F. Harrington and J.R. Mautz, Theory of characteristic modes for conducting bodies, IEEE Trans Antennas Propag AP-19 (1971), 622–628.
37. R.F. Harrington and J.R. Mautz, Computation of characteristic modes for conducting bodies, IEEE Trans Antennas Propag AP-19 (1971), 629–639.
38. C.T. Famdie, W.L. Schroeder, and L. Solbach, Numerical analysis of characteristic modes on the chassis of mobile phones, In: Proc. 1st European Conference on Antennas and Propagation—EuCAP 2006, Nice, France, 2006.
39. S.R. Best, The inverse relationship between quality factor and bandwidth in multiple resonant antennas, In: IEEE Antennas and Propagation Society International Symposium, Albuquerque, NM, 2006, pp. 623–626.
40. J. Anguera, C. Puente, C. Borja, G. Font, and J. Soler, A systematic method to design single-patch broadband microstrip patch antennas, Microwave Opt Technol Lett, 31 (2001), 185–188.
41. A. Andújar, J. Anguera, and C. Puente, A systematic method to design broadband matching networks, In: European Conference on Antennas and Propagation—EuCAP 2010, Barcelona, Spain, 2010.
42. R.C. Hansen, Fano limits on matching bandwidth, IEEE Antennas Propag Mag 47 (2005), 89–90.

AN ETCHED OPTICAL FIBER AS A VIBRATION SENSOR

Putha Kishore, Dantala Dinakar, P. Vengal Rao, and K. Srimannarayana
National Institute of Technology, Warangal, Andhra Pradesh, India; Corresponding author: kishorephd.nitw@gmail.com

Received 6 May 2012

ABSTRACT: *A center-etched single-mode fiber is designed as a vibration senor to monitor the vibrations of a simply supported beam. The sensor works on transmission power loss due to the mode volume mismatch and flexural strain of the fiber due to the bending in the fiber with respect to the bending of the beam. The sensor has high linear response to axial displacement of about 0.8 mm with sensitivity of 32 mV/10 μm strain. The simple design, small size, immune to electromagnetic interference (EMI), and flexible length are all added advantages that may find a place in industry to monitor the vibrations of the beam structures and bridges.* © 2012 Wiley Periodicals, Inc.
Microwave Opt Technol Lett 55:75–79, 2013; View this article online at wileyonlinelibrary.com. DOI 10.1002/mop.27240

Key words: *optical fiber; etched fiber; simply supported beam; vibration sensor; health condition monitoring*

1. INTRODUCTION

Now-a-days, the structural beams are used in all branches of engineering and science, mainly for civil, mechanical, nuclear power plants, opto-chemical monitoring, and industrial structures. Simply supported beams are one of the important structures in real life. The dynamic vibration response of a beam with time and frequency analysis gives enough information about the structural imperfections [1, 2]. Generally, in real time, the forces are nonperiodic and or suddenly released forces [3]. The conventional structural health-monitoring systems do not respond immediately for the damages and also they are affected by electromagnetic waves. Conversely, fiber optic sensing systems are not affected by electromagnetic waves and the material of the sensor is anticorrosive. Fiber optic sensors have been shown to be capable of measuring a variety of parameters including bending with high sensitivity and stable even at high temperatures [4, 5].

The aim of the present work is to design an inexpensive fiber optic vibration sensor to monitor the dynamic response of the rectangular simply supported beam with symmetric overhang. The sensor works on the principle of intrinsic intensity modulation corresponds to a force applied at the center of the beam, where etched portion of the sensing fiber is attached. The system is tested for the applied and suddenly released forces. The sensor has advantages of simple design, flexible length, and immune to electromagnetic interference (EMI), which enables to

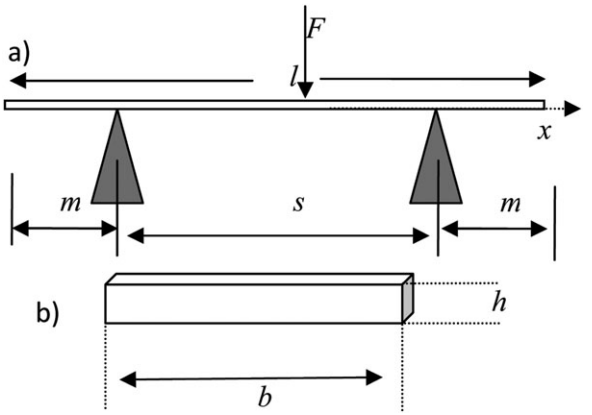

Figure 1 (a) Geometry of the simply supported beam and (b) cross section of the beam

replace the electronic sensors to avoid the electrical damages, easily imbed in composite structures and small in size.

2. THEORY OF SIMPLY SUPPORTED BEAM

A simply supported beam of thickness "*h*," width "*b*," and length of "*l*" with symmetric overhang of "*m*" is considered and carried out the experiments to measure the vibration of the beam using fiber optic vibration sensor. The geometry of the beam is shown in Figure 1.

The effects of shearing, rotatory deformations are ignored as the cross-sectional dimensions are constant and small in comparison to its length. Here, the transverse vibration of the beam is considered as a one degree problem [6–8]. The lateral displacement of the beam along the length for concentrated force or load applied at the center is expressed as [9]:

$$y = \frac{Fx}{12EI}\left(\frac{3l^2}{4} - x^2\right) \quad \text{for } 0 < x < \frac{l}{2} \tag{1}$$

$$y = \frac{F}{12EI}\left(x^2 + \frac{9xl^2}{4} - \frac{l^3}{4} - 3lx^2\right) \quad \text{for } \frac{l}{2} < x < l. \tag{2}$$

The bending of the beam at the center where the force or load applied is given as:

$$y_{\max} = \frac{F}{4Eb}\left(\frac{l}{h}\right)^3. \tag{3}$$

The free transverse vibration of the simply supported beam corresponds to concentrated load at the center and is expressed as [10]:

$$y(x,t) = \sum_{n=1}^{\alpha} \frac{2Fl^3}{n^4\pi^4 EI} \sin\left(\frac{n\pi}{2}\right) \sin\left(\frac{nx\pi}{l}\right) \cos(w_n t) \tag{4}$$

where w_n is the natural frequency of the overhang beam and is given by

$$w_n = \left(\frac{2\pi}{s}\right)^2 \sqrt{\frac{EI}{A\rho}} \tag{5}$$

where E, I, ρ, and A are the modulus of elasticity, moment of inertia, mass density, and cross-sectional area of the beam, respectively.

When the force is applied to center of the beam and it is released suddenly, the vibration of the beam undergoes a damped motion following a near step and giving the overshoot that slowly decays exponentially toward zero of the amplitude of vibration due to the structural damping of the beam and is given by [11]

$$y_d(x,t) = \sum_{n=1}^{\alpha} \frac{2Fl^3}{n^4\pi^4 EI} \sin\left(\frac{n\pi}{2}\right) \sin\left(\frac{n\pi x}{l}\right) \cos(w_d t) \exp(\xi w_n t) \tag{6}$$

where w_d and ξ are the damping frequency and the structural damping coefficient of the beam and are expressed as

$$w_d = w_n\sqrt{1-\xi^2} \quad \text{and} \quad \xi = \frac{y_{\max}}{\sqrt{4\pi^2 + y_{\max}^2}}. \tag{7}$$

3. ETCHED FIBER AS A SENSOR

An unetched fiber is less sensitive to macrobending when compared with an etched fiber. Thus, to enhance the sensitivity for macrobending, the fiber is chemically etched at the center. When the fiber is stretched, the reduction in the cross-sectional area leads to change in refractive index due to the photoelastic effect.

The change in core radius and index leads to a change in mode volume proportional to the induced tensile strain [12]. Therefore, the smaller cross-section and refractive index changes of the etched fiber results a larger strain and mode volume mismatch than that of an unetched fiber. For etched fiber, the refractive index of the cladding layer is higher than that of the surrounding air and the whole fiber can be regarded as a multimode fiber because of the strong reflection and recoupling with the propagating light within the core [13]. When the etched fiber experience a macrobending, the mode volume mismatch between the etched and the unetched portions of fiber causes transmission power loss due to the flexural strain (field strength). The mode volume mismatch increases as the macrobending of the fiber increases and the intensity of light received by the photo detector decreases within the limits of bending.

In general, two well-known methods to reduce the fiber diameter are D-shaping and chemical etching. Among them, chemical etching method is well controllable and is a easy technique. The general telecommunication fiber of 9/125 μm core/cladding is wet etched by the chemical method at the middle of the fiber. The protective plastic coating of length 1 mm is stripped off and then immersed in 40% of hydrofluoric acid solution for 30 min, which results in the fiber diameter to be remained at 50 μm. The etching is monitored in real time by measuring the transmitted power at 1540.32 nm FBG peak, and the power reduces rapidly when the evanescent field is reached. Once the etching process is terminated, the fiber is cleaned by distilled water and ethanol to release the remaining hydrofluoric acid and then dried under vacuum [14, 15]. Figure 2 shows the optical microscope photograph of the unetched and etched parts of the fiber.

4. EXPERIMENT

The schematic of the experimental setup is shown in Figure 3. It consists of a spring steel beam with $l = 308$ mm, $b = 25$ mm, and $h = 0.5$ mm, and it is overhung on two rigid bases with $m = 6.4$ mm, a broad band source of 1550 nm, a circulator, a FBG of peak wavelength 1540.32 nm at room temperature, a

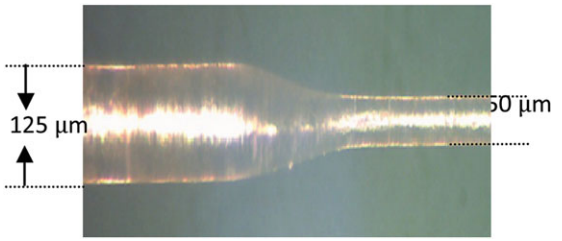

Figure 2 The unetched and etched parts of the fiber. [Color figure can be viewed in the online issue, which is available at wileyonlinelibrary.com]

matched photo detector with transimpedance amplifier circuit, and a data acquisition system. A center-etched fiber is attached at the center of the beam with an adhesive. The light couple from the broad band source is transmitted from the first node to the second node of the circulator and then through the FBG.

An index matching gel is used to minimize the noise level and reflection from the end of the fiber. The reflected peak of the FBG is transmitted from node 2 to node 3 and then through the etched fiber.

The load is applied at the center of the spring steel beam in terms of the bending, where the etched fiber is attached. The axial bending is applied to the beam in steps of 50 μm and measured the response of the sensor as shown in Figure 4. The spectral response characteristic of the sensor for different lateral displacements is as shown in Figure 5. The sensor has high linear response to axial displacement of 0.8 mm with sensitivity of 32 mV/10 μm strain.

5. RESULTS AND DISCUSSION

The beam is subjected to bending periodically with the stepper motor attached a cam with some offset and recorded the response of the sensor with the data acquisition system shown in Figure 6. The offset portion in Figure 6 shows the stability of the signal. The sensor is tested for the vibration of the beam for applying the force at the center and released suddenly as shown in Figure 7. The exponential decay of the amplitude of vibration of the beam after releasing of force is agreed with the theoretical response. In Figure 7, from the points *a* to *b*, the beam is excited by the near step force and then it overshoots to underdamped motion due to the structural damping and slowly it comes to zero amplitude of vibration with the time. The fast Fourier transform (FFT) of time domain signal gives the frequency of vibration of the beam and it is found to be 17 Hz, which is matched with theoretical value from Eq. (7). The time and frequency response of the beam gives the sufficient information to know the health condition of the beam. The sensor is also tested for the suddenly released step force applied repeatedly and the response is as shown in Figure 8. As the length of the sensor plays an insignificant role in power loss, it is recommended for real-time health-monitoring systems.

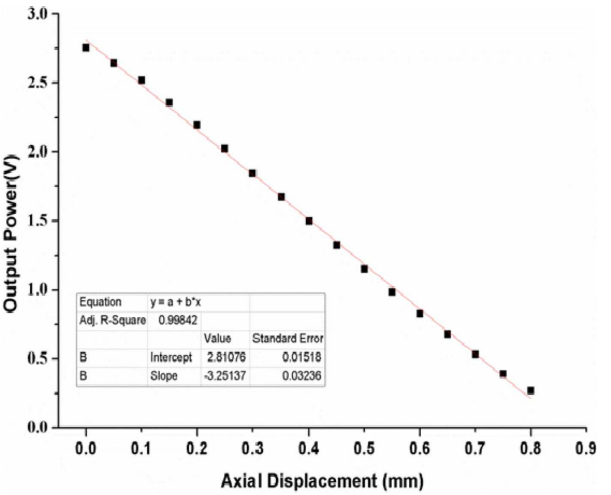

Figure 4 The sensor response for axial displacement of the beam at the center. [Color figure can be viewed in the online issue, which is available at wileyonlinelibrary.com]

6. CONCLUSION

A simple fiber optic vibration sensor was designed and demonstrated to monitor the health condition of the simply supported beam with symmetric overhang. The sensor shows high linear

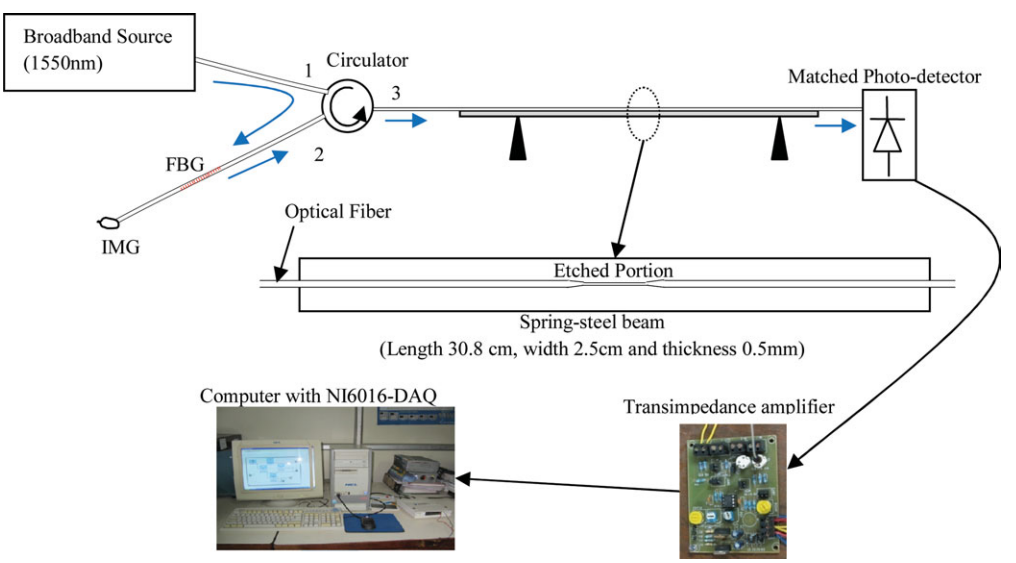

Figure 3 The schematic experimental setup of the etched vibration sensor. [Color figure can be viewed in the online issue, which is available at wileyonlinelibrary.com]

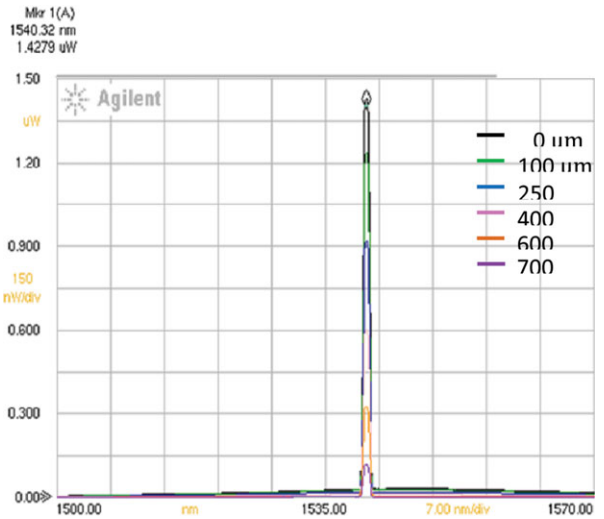

Figure 5 The optical spectrum of the fiber at different axial displacements of the beam. [Color figure can be viewed in the online issue, which is available at wileyonlinelibrary.com]

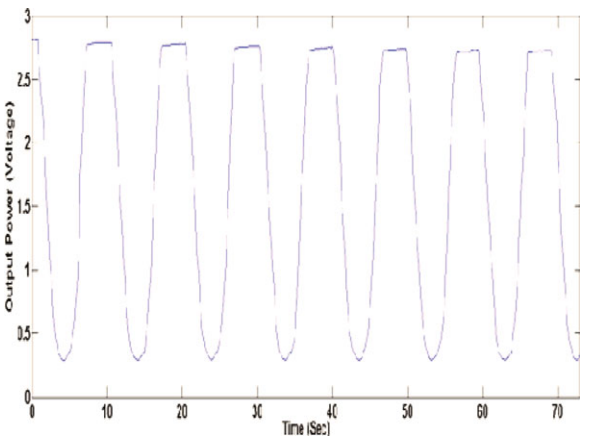

Figure 6 Response of the sensor for periodic vibration of the beam. [Color figure can be viewed in the online issue, which is available at wileyonlinelibrary.com]

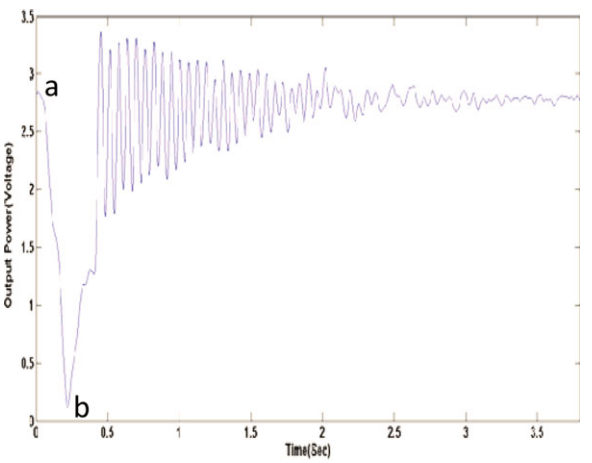

Figure 7 Response of the sensor for suddenly released force at the center of the beam. [Color figure can be viewed in the online issue, which is available at wileyonlinelibrary.com]

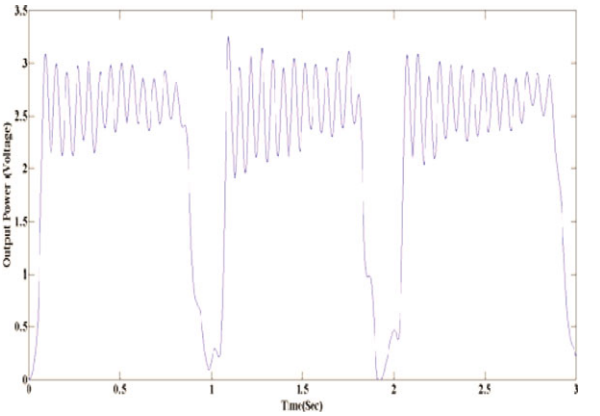

Figure 8 Repeatedly applied force to the beam and response of the sensor. [Color figure can be viewed in the online issue, which is available at wileyonlinelibrary.com]

response of 0.8 mm axial displacement with sensitivity of 32 mV/10 μm strain. The sensor was tested for forced vibrations of the beam such as suddenly released forces and periodic force, which would be more realistic and appropriate for real field. The time response of the beam was recorded and measured the frequency response using FFT. This gives enough information about the state of the beam and failures. The sensitivity of the sensor can be changed and it depends on the diameter of the etched fiber by reducing the clad diameter using chemical etching method. The sensor has its own advantages such as simple design and analysis, economical, flexible length, and small size. These advantages enable the sensor for remote monitoring of the beam-like structures.

REFERENCES

1. J.-D. Yau, Vibration of simply supported compound beams to moving loads, J Mar Sci Technol 12 (2004), 319–328.
2. W. Dongi, L. Tong, and Y. Zhaoqing, The simulated analysis based on EMD and shape factor to identify damage location of a simple supported beam steel bridge, In: International Conference on Digital Manufacturing & Automation, 2010, pp. 808–810.
3. L. Meirovitch, Elements of vibration analysis, 2nd ed., McGraw-Hill Pvt. Ltd., New York, NY, 1986.
4. K.S.C. Kuang, W.J. Cantwell, and P.J. Scully, An evaluation of a novel plastic optical fiber sensor for axial strain and bend measurements, Meas Sci Technol 13 (2002), 1523–1534.
5. C.H. Chen, Y.L. Shen, and C.S. Shin, Using distributed Brillouin fiber sensor to detect the strain and cracks of steel structures, J Mech 26 (2010), 547–551.
6. J.F. Murphy, Transverse vibration of a simply supported beam with symmetric overhang of arbitrary length, J Test Eval 25 (1997), 552–524.
7. S.M.J. Ali and Z.S. Al-Sarraf, Study the transverse vibration of beam with different length, Al-Rafidain Eng J 17 (2009), 83–91.
8. S. Timoshenko and D.H. Young, Vibration problems in engineering, 3rd ed., East-West Press Pvt. Ltd., 1964.
9. W.A. Nash, Schaum's outline of theory and problems of strength of materials, 4th ed., McGraw-Hill Pvt. Ltd., 1998.
10. S.M. Abdullah, Free vibration of simply supported beams using Fourier series, Al-Rafidain Eng J 14 (2006), 51–67.
11. S.G. Kelly, Fundamentals of mechanical vibrations, International Editions, McGraw-Hill Pvt. Ltd., 1993.
12. M. Vaziri and C.-L. Chen, Etched fibers as strain gauges, J Lightwave Technol 10 (1992), 836–841.
13. Y. Zaatar, D. Zaouk, J. Bechara, A. Khoury, C. Llinaress, and J.P. Charles, Fabrication and characterization of an evanescent wave fiber optic sensor for air pollution control, Mater Sci Eng B 74 (2000), 296–298.

14. X. Tian, X. Cheng, W. Qiu, Y. Luo, Q. Zhang, B. Zhu, and G. Zou, Optically tunable polarization state of propagating light at 1550 nm in an etched single-mode fiber with azo-polymer overlay, IEEE Photonics Technol Lett 23 (2011), 170–172.
15. P. Wang, Q. Wang, G. Farrell, G. Rajan, T. Frier, and J. Cassidy, Investigation of macrobending losses of standard single mode fiber with small bend radii, Microwave Opt Technol Lett 49 (2007), 2133–2138.

BROADBAND PRINTED PLANAR MONOPLE ANTENNA FOR WIRELESS TERMINAL DEVICES APPLICATIONS

Jwo-Shiun Sun and Sheng-Yi Huang
Graduate Institute of Computer and Communication Engineering, National Taipei University of Technology, Taipei, Taiwan;
Corresponding author: t5419018@ntut.org.tw

Received 8 April 2012

ABSTRACT: *In this study, the compact broadband printed planar monopole antenna is presented for wireless communication devices applications, which is designed to work in 2.4–4.2 and 4.8–5.9 GHz in which it is suitable for Wimax, WLAN, WiFi, and Bluetooth. The ratio of impedance bandwidth of the presented antenna to the central frequency bands of 3.3 and 5.3 GHz is as high as 1.8:1 (BW% = 54.5 and 20.6%, respectively). The total volume of the presented antenna is 45 (*L*) × 40 (*W*) × 0.4 (*H*) mm³, and the antenna gain is 3.0–6.2 dBi in the resonant frequency bands. The experimental results in general agree with the simulated data by high-frequency structure simulator.* © 2012 Wiley Periodicals, Inc. Microwave Opt Technol Lett 55:79–82, 2013; View this article online at wileyonlinelibrary.com. DOI 10.1002/mop.27272

Key words: *Wimax; WiFi; WLAN; antenna gain; monopole*

1. INTRODUCTION

Antenna acts as an important role in wireless communication system to transmit and receive electromagnetic (EM) emission energy. Furthermore, the characteristics of compact, low profile, easy fabrication, wideband, and low specific absorption rate are attractive for wireless communication applications. Planar inverted-F antennas (PIFAs) meet the feature of compact, but they still occupy a quite large space due to the three-dimensional (3D) structures of feeding and shorting pins [1–7]. Planar antenna, in contrast to PIFAs, is a good choice due to no 3D structures, which is applicable to be fabricated into the devices of which the space is limited.

Several research literatures about the planar antenna with various feeding structures have been proposed. Wrapped and folded planar monopole antennas with planar feeding structures are presented [8, 9], which have the characteristics of wideband, omnidirectional patterns, and compact size, but they still occupy a large space. Planar monopole antennas with side-feeding structure [10] and/or trapezoidal feeding structure [11] are presented, which have the characteristic of compact size, but increase the manufacturing difficulties and cost.

Here, the presented antenna has the quite simple configuration that is made by the twofold: (1) A patch prototype is conducted to determine the lower resonant band of 2.4 GHz; then, cut and/or modify the patch antenna to form a shape of capital C, which is no compromise of return loss. (2) A planar conducting strip is added inside the radiator of capital C shape to induce the higher resonant frequency band of 5 GHz by mutual coupling. An open-end stub is applicable for tuning the impedance matching covered the specified bands as referred to the modification concept of nonsymmetrical parallel short circuit [12].

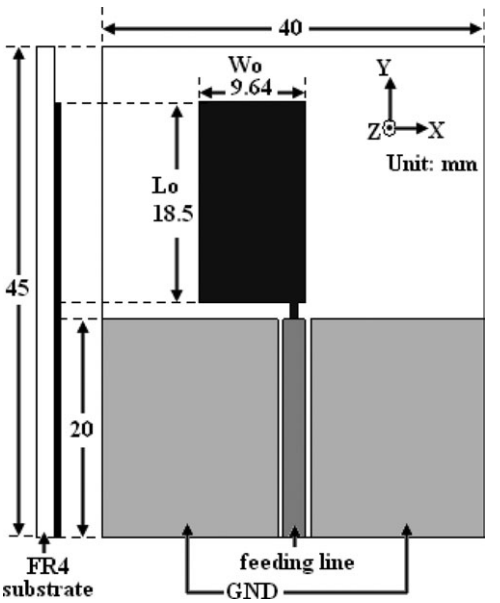

Figure 1 Original prototype configuration of patch antenna for the lower resonant frequency band of 2.4 GHz

The total volume of the presented antenna is 45 (*L*) × 40 (*W*) × 0.4 (*H*) mm³, which the detailed geometry is illustrated in Section 2. The characteristics of the far-field omnidirectional radiation patterns and antenna gain are attainable and the experimental results in general agree with the simulated data by high-frequency structure simulator (HFSS), which will be illustrated in Section 3.

2. ANTENNA DESIGN AND CONFIGURATION

A material flame retardant 4 (FR4) with the relative permittivity (ε_r) of 4.4 and the dielectric loss tangent (tan δ) of 0.02 is adopted to be the substrate structure of the presented antenna, of which the volume is 45 (*L*) × 40 (*W*) × 0.4 (*H*) mm³. The feeding coplanar waveguide is adopted due to having the good characteristics of easier getting the impedance matching to increase the impedance bandwidth [13, 14]. As shown in Figure 1, an original patch prototype is made by equation as (1) referred to Ref. 15 for the lower resonant frequency band of 2.4 GHz; where *c* denotes the velocity of light (3×10^8 m/s), *L* and *W* denote the length and width of a radiator element, and f_0 denotes the resonant frequency.

$$f_0 = \frac{c}{4(L+W)} \tag{1}$$

The design condition of one-quarter wavelength is adopted to make a compact antenna and a trial simulation is adopted in HFSS to make an optimizing configuration. Therefore, the dimension of ($L_o + W_o$) of the patch prototype is 28.14 mm approximately for 0.223-wavelength at 2.4 GHz. Then, cut and/or modify the original patch prototype to be a formation of capital C shape that is no compromise of S_{11} in the lower resonant frequency band. As shown in Figure 2, it illustrates the optimizing geometry of the presented antenna. As the denoted *W*, it is directly related to the performance of S_{11} in the lower frequency band of 2.4 GHz. Besides, a planar printed conducting strip (L_2) is added inside the radiator of capital C shape to induce the higher resonant frequency band of 5 GHz by mutual coupling. Definition of the original open-end stub W_2, it means that the